frontiers in Earth Science

HYPOTHESIS AND THEORY
published: 21 January 2022
doi: 10.3389/feart.2021.824755

Nyexon Rock Avalanches: A Special Intrusion Restraint Mechanism, Tibet, China

Jie Cui[1], *Chunyu Gao*[2,3]*, *Zhilong Zhang*[2,3], *Guifu Xiang*[1], *Xiong Liu*[1] *and Ye Huang*[2]

[1]School of Environment and Resource, Southwest University of Science and Technology, Mianyang, China, [2]College of Water Resource and Hydropower, Sichuan University, Chengdu, China, [3]State Key Laboratory of Hydraulics and Mountain River Engineering, Sichuan University, Chengdu, China

The Nyexon Rock Avalanches in the southern Qinghai-Tibet Plateau is a huge scale earthquake-induced slope disaster in the Holocene, the accumulation area has distinct sedimentological characteristics, which is of great significance for studying the intrusion and restraint mechanism during long-distance transportation of large rock avalanches or debris avalanche. This long-distance transportation induced a series of landform types, such as ridges, hills, and ravines; they are widely distributed in all areas and extensively developed shear zones, jigsaw cracks, and other structures within the sedimentary structure. With the analysis of DEM data and geological survey, two main types of basement structures and their transition relationships are distinguished; they play an essential role in the restraining bottom during rock avalanches. In the sedimentary structure, the block facies and mixing facies occupy the main body of the deposition from the center to the distal area. Under the basement restriction, mixing facies are formed between the bottom of the sedimentary layer and the basement sedimentary structure; the shear band is mainly developed along with the mixing facies and basement facies, which is accompanied by basement liquefaction and rheology. A sedimentary facies model is established based on the sedimentary structure sequence of the Nyexon Rock Avalanches transportation. After analyzing the failure mechanism of the rock avalanches, it is believed that in the initial stage of failure, the rock avalanches is transformed into a particle flow that is similar to the debris avalanche, which is restrained by the basement structure and lateral bound; then, an accumulated obstacle highland is formed in the central area after deceleration, making the transportation of the main fluid to deflect quickly.

Keywords: rock avalanches, failure mechanism, intrusion constraint, transport processes, sedimentary structures

OPEN ACCESS

Edited by:
Xiaodong Fu,
State Key Laboratory of Geomechanics and Geotechnical Engineering, Institute of Rock and Soil Mechanics (CAS), China

Reviewed by:
Lei Zhu,
Chinese Academy of Sciences, China
Shunde Yin,
University of Waterloo, Canada

***Correspondence:**
Chunyu Gao
chygao@scu.edu.cn

Specialty section:
This article was submitted to Geohazards and Georisks, a section of the journal Frontiers in Earth Science

Received: *29 November 2021*
Accepted: *15 December 2021*
Published: *21 January 2022*

Citation:
Cui J, Gao C, Zhang Z, Xiang G, Liu X and Huang Y (2022) Nyexon Rock Avalanches: A Special Intrusion Restraint Mechanism, Tibet, China. Front. Earth Sci. 9:824755. doi: 10.3389/feart.2021.824755

1 INTRODUCTION

Since the Holocene age, many giant rock slides and rock avalanches have been active in the Qinghai-Tibet Plateau and the surrounding areas (Hewitt, 1999; Strom and Korup, 2006; Qi et al., 2011; Xu et al., 2012; Wang et al., 2017; Wang et al., 2018; Zeng el al., 2020). During the risk assessment of natural disasters in plateau areas, the kinematic study of large-scale rock slides and rock avalanches with exceptional mobility has received particular attention. The complete intrusion process of large rock avalanches or debris avalanches is rarely recorded. However, the well remained structure can still provide a common basis and references for related specific research on rock avalanches or debris avalanches.

In the present, there have been many discussions about the transportation and emplacement of rock avalanches or debris avalanches (Anma et al., 1989; Vallance and Scott, 1997; Takarada et al., 1999; Capra and Macias, 2000; Bernard et al., 2009; Hu et al., 2009; Roverato et al., 2015). Theoretical hypotheses on the cause of abnormal long-distance transport include the theory of inviscid particle flow, the theory of air cushion, and the theory of trapped air causing fluidization (Kent, 1966; Shreve, 1966; Hsü, 1975; Erismann, 1979; Davies, 1982; Sassa, 1988; Foda et al., 1994) etc. Nevertheless, there is still no universal mechanism or theory to explain all these types and phenomena (Orwin et al., 2004; Devies et al., 2011).

In addition to the rock nature and the initial transportation state, the main conditions or factors that constrain the long-distance transportation and placement of rock avalanches or debris avalanches include the basement surface undulation, significantly raised obstacle, foundation structure strength, water-bearing condition, etc. These factors will affect or limit the direction, speed, and form of flow transport during the transportation and placement of debris (Moore and Mathews, 1978; Davies, 1982; Evans, 1989; Evans et al., 1989; Erismann and Abele, 2001Clavero, et al., 2002; Pollet and Schneider, 2004; Jibson et al., 2006; Bernard et al., 2009; Huang et al., 2012; Weidinger et al., 2014; Dufresne et al., 2015). Almost all geomorphology and structure are reflected in the evolution process of sedimentary units, which result from the emplacement and restraint of rock avalanches. The detailed geological survey is helpful to reveal the intrusion mechanism of certain large rock avalanches or debris avalanches (Schilirò et al., 2019).

In order to evaluate the potential major slope disasters in major engineering activities under the impact of strong tectonic activity in the Qinghai-Tibet Plateau and to explore the long-distance abnormal emplacement process and restraint mechanism of large rock avalanches or debris avalanches, Nyexon rock avalanches in the southern Qinghai-Tibet Plateau were selected as the research subject. The Nyexon rock avalanche (NRA) is a kind of earliest studied slope hazard in the southern plateau, where active seismic activity exists (Armijo et al., 1986). The rock avalanche event occurred about 820 years ago (Zeng et al., 2020). Through field investigation, compared with the three different placement patterns of the usual rock avalanches or debris avalanches (Pier et al., 1991), as a specific large-scale rock avalanche, the L-shaped placement of the NRA is unusual, making Senai Village directly facing the slope escape from the disaster, but Nyexon Village is attacked under the condition of no obvious terrain restrictions on the transportation route. Therefore, the research on the NRA is valuable. Due to the rich and well-preserved accumulation landforms formed by the NRA, with the geological observation and mapping, the collapse mechanism, the effect of sedimentary characteristics on its placement, and the corresponding mechanism are deeply discussed, which is of specific significance for accurately evaluating and preventing the large-scale slope disasters in seismically active areas.

2 GEOLOGICAL SETTING OF NRA

Since the late Cenozoic, the south-north tectonic belts are developed significantly in the southern part of the Qinghai-Tibet Plateau (Armijo et al., 1986; Tapponnier et al., 2001; Taylor et al., 2003; Pan et al., 2006; Yin and Taylor, 2011), among which the Yadong-Gulu rift is the most active one (Wu et al., 2015). The rift zone on the north side of the Yarlung Zangbo suture zone expands into the Nyemo graben group consisting of seven graben bodies. The studied area is located in the Angang graben on the east side (**Figure 1**).

The Angang graben is a willow-like intermountain basin, where the main fault is located in the basin-mountain intersection on the west side of the basin (**Figure 1**), and the fault triangular face of the mountain front shows the activity of the graben structure. Besides, in this area, the seismic activity is frequent (Wu and Ye, 2009), the rock strata is mainly pale-colored, coarse-grained, two-cloud granites of the Paleogene (Wang et al., 2019), and the intrusive magmatic rock structures such as dark pyroxene homogenous enclaves, homologue enclaves, and band structures are well developed. In the Angang Basin, the sediments are formed through the cross-deposition effect among the glacial water deposits, piedmont alluvial fans, swamps, and rivers. From north to south, the swamp type gradually changes from alluvial fan swamps to river swamps. The weathered soil on the slope's surface and the colluvial deposits form slope wash facies with a great thickness. The bottom sediment of the basin is mainly demonstrated by modern fluvial deposits in the Xuqu River and swamp facies.

3 ANALYSIS METHODS

Considering the vast coverage of the NRA, the entire accumulation area was investigated with the route method, and the characteristics of the debris size, composition, provenance were drawn and statistics in detail. Moreover, along with the Xuqu River and Xiagaqu River, tens of exposed mounds, ridge morphology, basement structure, etc. were investigated and sampled in detail. In addition, in order to explore the accumulation and distribution of debris below the scar area, high-density electrical geophysical methods are used in the field to detect the area from the bottom to the proximal area of the scar area to investigate the characteristics of the basal structure and the water-bearing conditions.

Using high-resolution Google remote sensing images, the features of NRA and its surrounding area were drawn in detail from the aspect of the macro landscape; then, the spatial distribution sequence of mounds, ridges, and fractures was analyzed. In addition, the spatial distribution of huge breccias on the surface and the development law of particle size were also included.

As the basis for detailed geological observations, a quadrotor drone was used to capture image data with a resolution of 0.1 m and an area of 8.3 km^2 to create a digital elevation model (DEM). The ArcGIS software is adopted to establish macro-

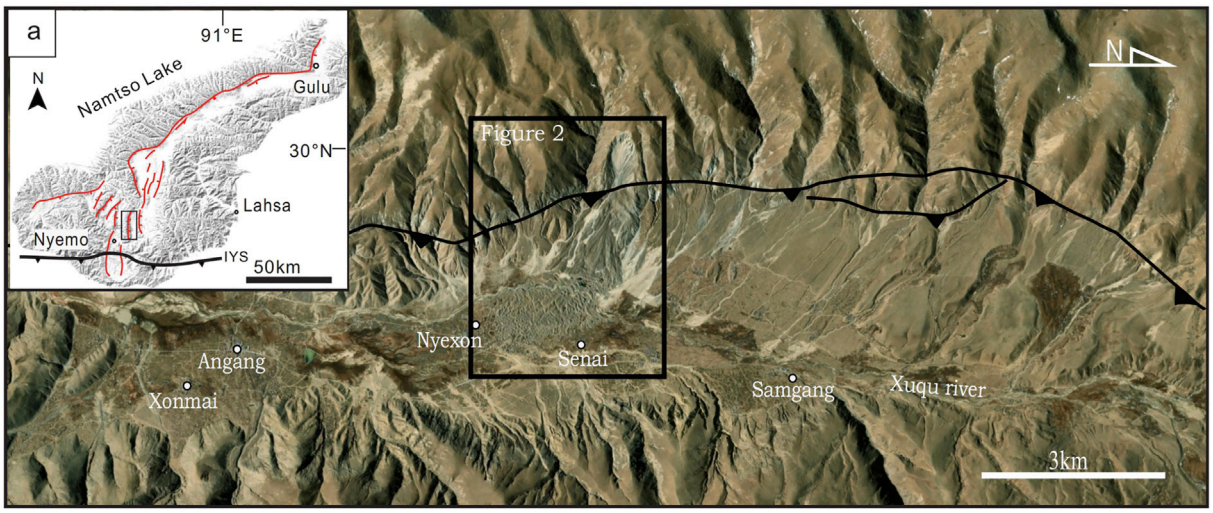

FIGURE 1 | Geological setting of the Angang Graben.

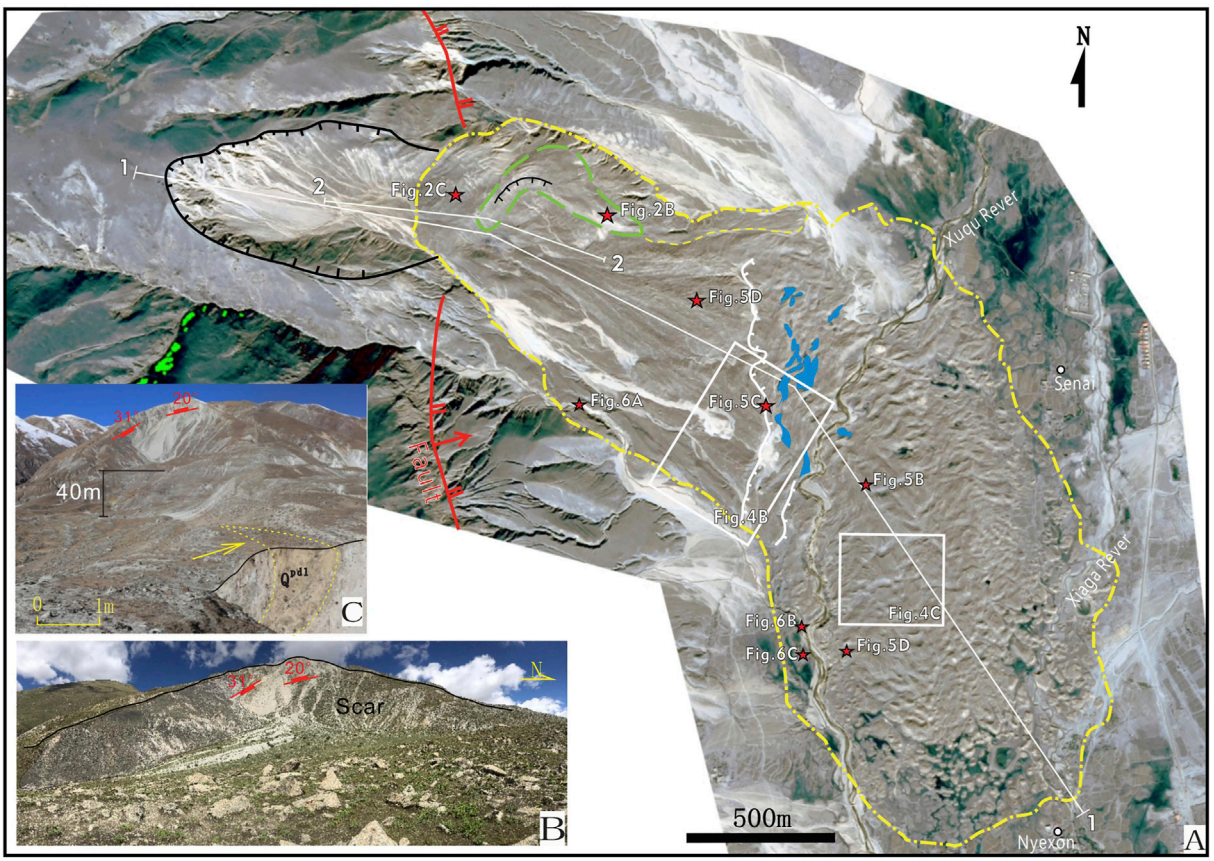

FIGURE 2 | Remote sensing image map of the Nyexon Rock Avalanches. **(A)** Plan view of the NRA loaded, yellow line for the NRA sedimentary area, green line for the undeposited area, and black line for the scar area, with **(B)** view of its scar area. **(C)** A high escarpment formed by lateral erosion of the original ridge and foot on the left.

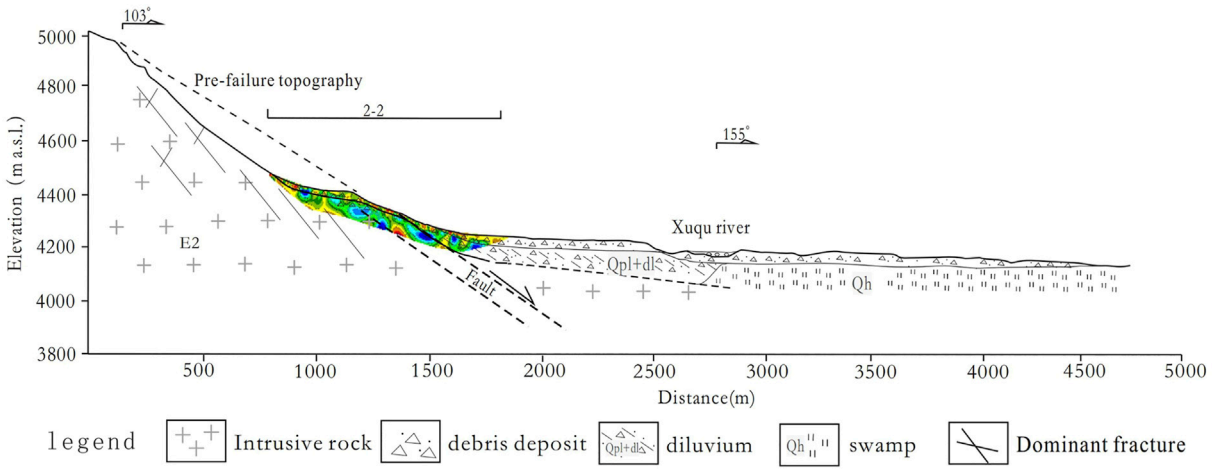

FIGURE 3 | Longitudinal profile of the NRA. Number 2-2 is the geophysical prospecting section line number.

topographic indicators, in which the focal statistic method is used to calculate the topographic undulations of the accumulation area. Moreover, by carefully describing the development and distribution of hills, ridges, and faults, it reflects the internal relationship between the transportation sequence of debris and the accumulation structures. While investigating the source of the detrital material in the field, according to the formation cause, the detribalization characteristics of different weathering degrees were distinguished, and the mixing degree of the base material components in each area was determined; according to the sedimentary structure and topography, the type and transition characteristic of sedimentary facies belts in each region are categorized. Finally, considering the interaction between the debris accumulation and the basement, the mechanism of the debris avalanche placement process, the high-fluidity emplacement process, and the constraining factors, are discussed.

4 RESULT

4.1 General Characteristics of NRA

NRA comes from the thick and tall granite mountains on the west side of the Angang Graben, where the protruding ridges sandwiched by gullies form the original landform. In this area, the normal faults across the bottom of the slope and huge piedmont landslides develop above them. The debris caused by the rock avalanche covers a range of about 4.68 km^2 from the gentle slope of the mountain front to the bottom of the flat valley. The horizontal distance from the scar area to the far end is 4.67 km, the height difference of the transportation path is 890 m, and the overall slope is 110‰. The plane morphology of the accumulation area shows that during the rock avalanches transportation, the starting location is 105°, and it quickly deflects southward to 155° after passing the Xuqu River (**Figure 2A**). However, the coverage width is 0.9–1.4 km, which means that compared with the transportation in the main direction, the horizontal expansion of fluid did not occur significantly.

The detrital material in the rockfall accumulation area is mainly composed of granite debris from the scar area and the material mixed in the basement with the transportation. The clastic particle ranges from boulders to clay, and it also contains the peat layer with rich organic matter in river swamp facies (**Figure 3** and **Figure 6E**).

Considering the expansion of the original source of the rock avalanche and the proportion of the substrate material during the transportation, it is relatively reasonable to estimate the disaster of the space volume of the scar area. Due to the uncertainty of the original slope morphology of the scar area, its original surface morphology of the scar area is reconstructed based on the assumption that the surface morphology still keeps the original shape, and the disaster scale is estimated to range from 27.5×10^6 m^3 to 35.8×10^6 m^3.

4.2 Scar Area

The entire scar area is composed of the head cliff, two lateral slopes, and the bottom surface (**Figure 2**). At the front edge of the scar area, a steep slope belt with a height of 90 m is developed, the topography at the exit section is extremely complex; at the trailing edge of the slope, a geomorphic uplift zone is formed, below where the front edge of the slope is mainly covered by primitive collapsing deposits (**Figure 2B**), forming a very convex ridge, which gradually descends and extends eastward about 0.7 km.

The upper rock mass structure of the scar area is mainly controlled by two main groups of wedge-shaped bodies that are composed of dominant fissures (**Figure 2C**). Because the bottom area is affected by the regional fault structure, a densely dipping fissure zone develops in the bedrock area (Wang et al., 2019).

At present, in the scar area, only the bottom area is covered by debris with different thicknesses. The results of geophysical exploration show that the burial depth of the damaged bottom bedrock is 5–20 m, and the morphology is generally gentle; at the same time, the low conductivity area shows that the width of the

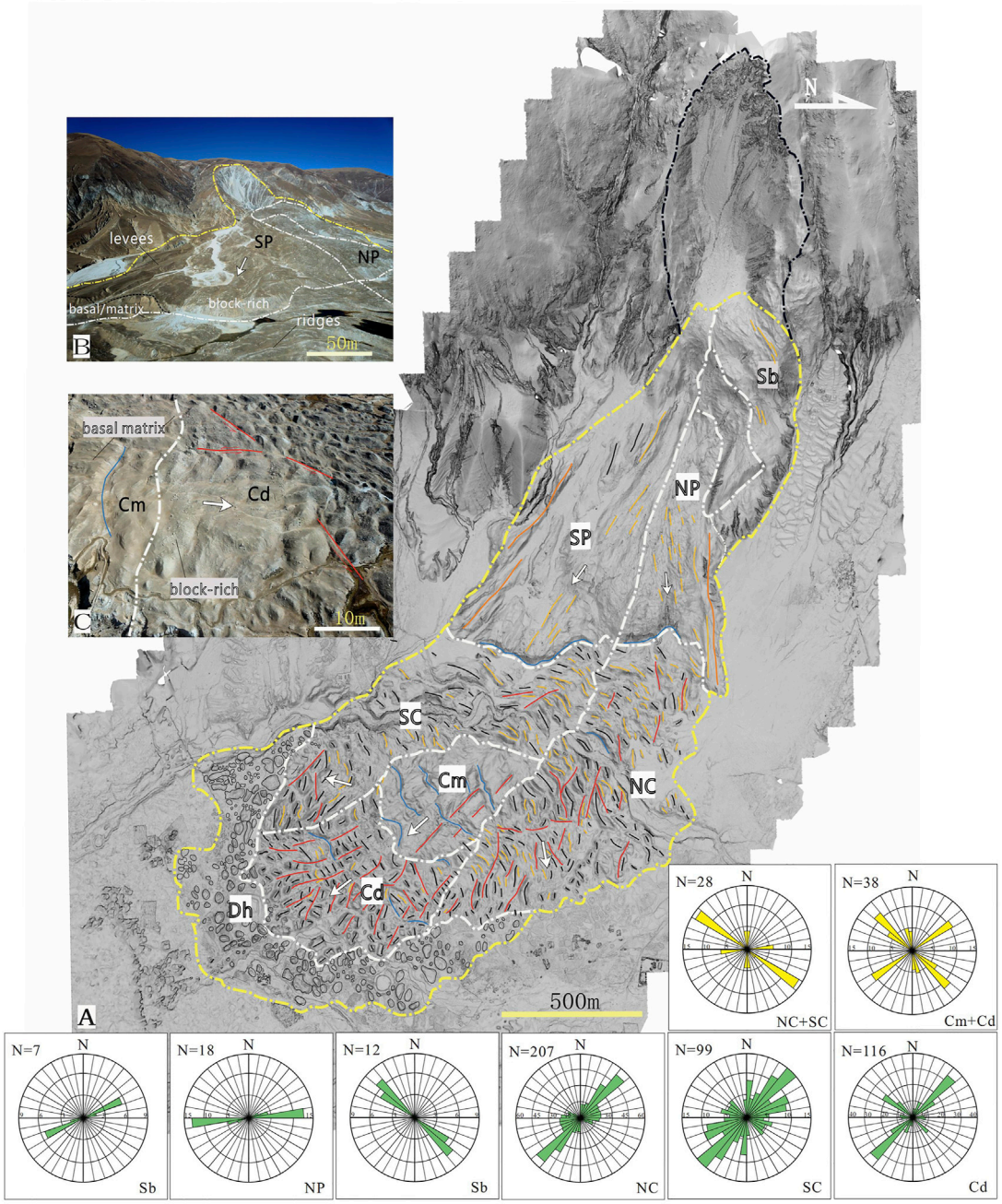

FIGURE 4 | (A) Shaded relief map of the NRA showing zones and subzones, accumulation area on the east side contains eight facies' intervals. White dashed line is the partition line, red dashed line is the ground fracture, black dashed line is the direction of the mound, yellow dashed line is the direction of the ridge. White arrow is the direction of movement, and range line is the direction of the levees. Green rose diagram is the ridge and hill, yellow rose diagram shows the location of the point break. **(B)** Drone top view of the proximal area, two different longitudinal mounds, black is the boundary of the sedimentary structure. **(C)** Drone top view of the central area, red is the direction of the surface fault.

affected zone of the bottom fault layer is more than 40 m, and the current fault zone is in a water-rich state (**Figure 3**). According to the on-site investigation, the ridge is not completely destroyed, and most of the deposits in the middle and lower parts are retained. Moreover, erosion also causes a steep slope zone on the left side of the ridge in the lateral direction (**Figure 2B**).

4.3 Structure

In the proximal area, NRA retains massive survivors and significant breccia accumulations on the surface; in the distal area, it forms a mixing facies structure similar to detrital avalanches, whose macroscopic accumulation forms include hummocks, ridges, scarp, trenches and levees, etc. The

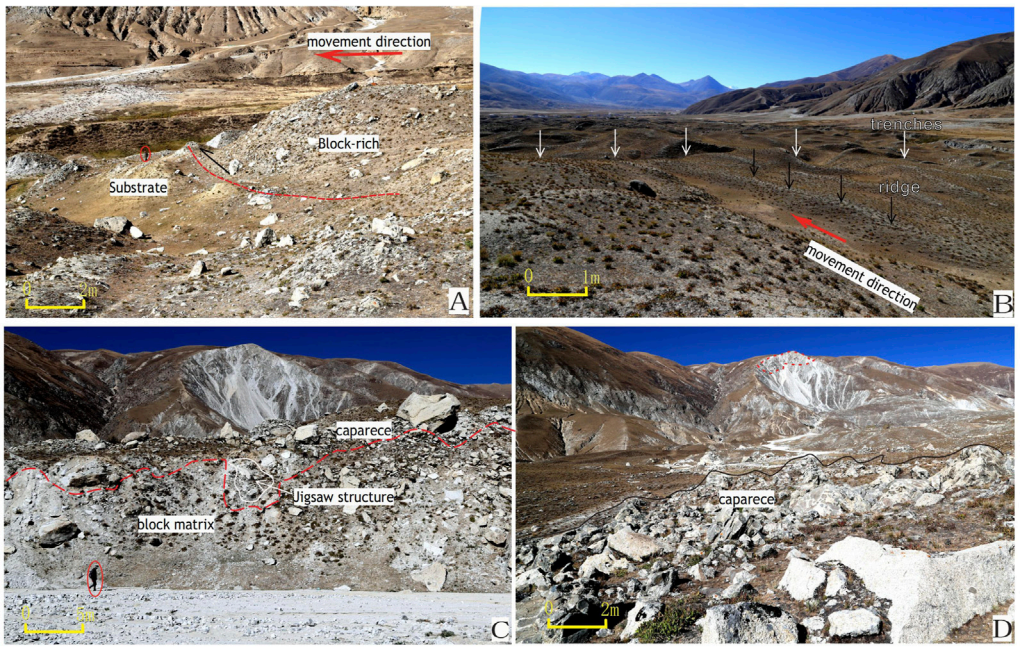

FIGURE 5 | The features of the sedimentary structure of the NRA. **(A)** Contact features of the block facies and the basement in the central area. **(B)** Transverse grooves and ridges in the central area. **(C)** Cross-sectional structure of the carapace facies at the front edge of the longitudinal mound. **(D)** Plane deposition range and the potential source area of the block are inferred to be the red range in the middle and upper part of the scar.

accumulation area of NRA is divided into different structural units, and the corresponding relationship between internal structure and macro-topography is reflected through the detailed description (**Figure 4A**).

4.3.1 Hummocks

The morphology of mounds includes longitudinal hummocks, round mounds, and transition types. Longitudinal hummocks are distributed from the proximal end of the scar area to the scarp belt near the Xuqu River (**Figure 4B**). Along the left side of the central line, the longitudinal hummocks are divided into two uplift belts arranged coaxially; the uplift amplitude increases toward the front edge, forming levees on the outer edge of the distal region of the longitudinal hummocks (**Figure 4A**).

In the proximal area of the scar area, except for the main debris accumulation part of the two longitudinal hummocks in the left area, in the center of the proximal end and the limited range of the right ridge, a more critical debris longitudinal mound is retained (**Figure 4B**). Through the inversion analysis of the slope map processed by the DEM, it is found that this area is macroscopically a gentle trough inclined from both sides to the center, and several parallel low-undulating longitudinal hummocks are developed at the bottom and inside (**Figure 4B**). Therefore, it is inferred that the placement process of the debris is in the proximal region. The piedmont alluvial fan acts as the base emplacement process, making the base structure undergo strong compression and deformation and inducing a mixed accumulation zone of the base on the further right bank of the xuqu; at the same time, the section of cliff in the front area shows the obvious high-angle contact relationship between the clastic matrix accumulation and the laterally uplifted alluvial fan fine-grained sedimentary layer, showing the intrusion mode of the proximal central area (**Figure 4B**).

From the center to the far end of the left bank of the Xuqu River, the shape of the mounds mainly includes long mounds, round mounds, shield mounds, etc. The plane morphology of their arrangement is affected by the fracture and appears to be more fragmented, forming coaxial parallel train hummocks (**Figure 4C**). However, suppose the influence of lateral fracture is not considered. In that case, the front-end mound train occurs slight vertical expansion in the form of a stream zone (Belousov et al., 1999), indicating that even under the constraining effect of the structure of the substrate, the variation of flow velocity in the front-end area is almost insignificant. In the farthest area, the thickness of the debris accumulation is very thin (**Figure 5A**), and in the bottom structure dominated by shear bands, the content of fine particles increases, and the distribution of mounds become more isolated.

4.3.2 Ridge

Ridge is the uplifted landform similar to the hill, and they can be distinguished according to the Overall aspect ratio, the aspect ratio of the former is generally greater than 1.5 (Dufresne and Davies, 2009). As for ridges in the NRA accumulation area, they are mainly characterized by steep slopes and sharp ridge tops. According to the direction of the ridge top line, they are defined as transverse ridges and longitudinal ridges. The former intersects

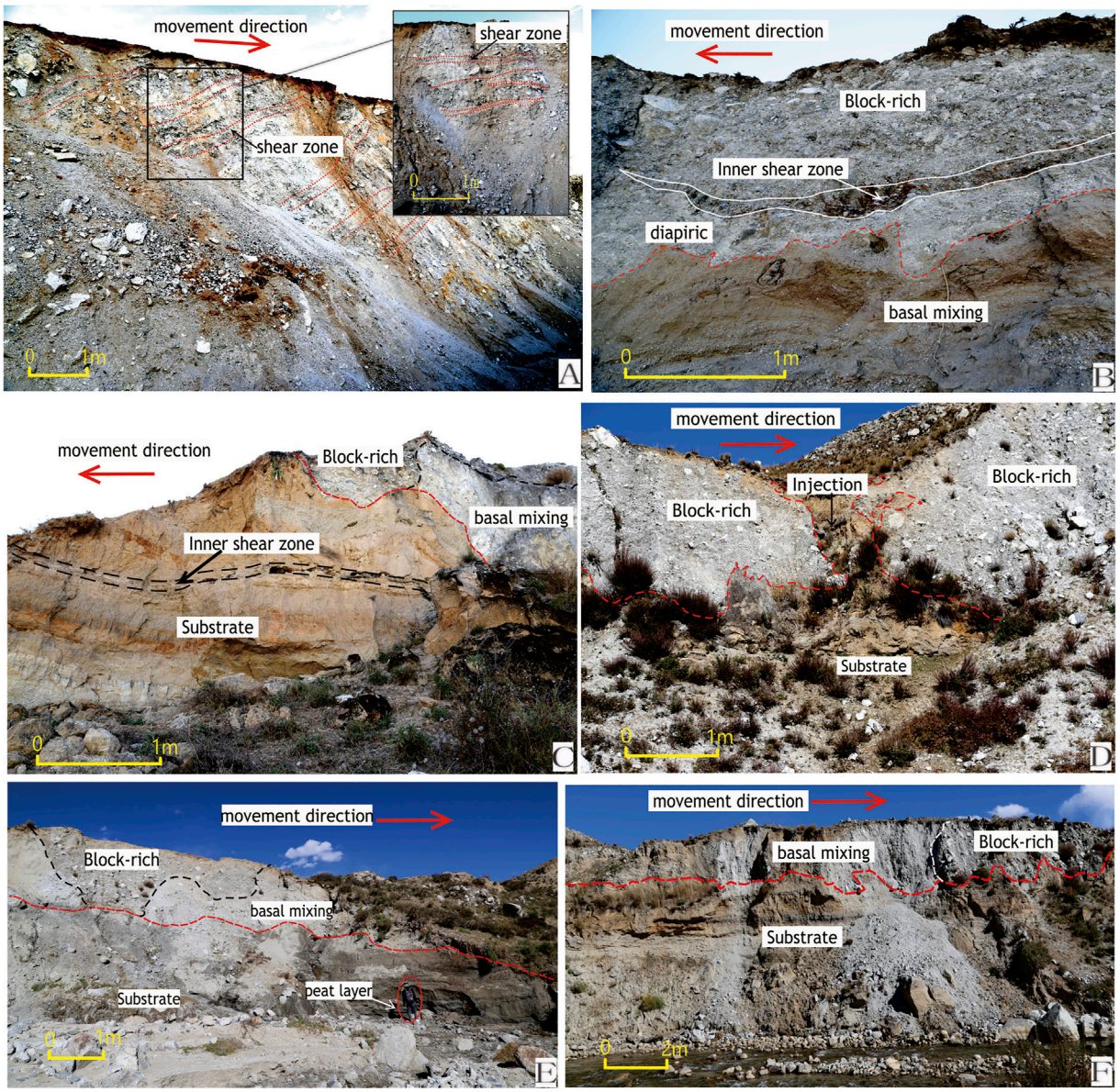

FIGURE 6 | The characteristics of sedimentation reflected by NRA on-site photographs. **(A)** Multiple shear zones and detailed features. **(B)** Rheological and shear phenomena of the sedimentary bottom layer. **(C)** Horizontal shear zone and diapir structure inside the basement. **(D)** Injection structure. **(E)** Outside the central area. The contact relationship between the horizontal deposition of the peat-bearing marsh facies and the clastic deposition. **(F)** Clastic deposition thickness in the distal area and the diapir structure inside the basement.

the main direction of transportation at a large angle. Lateral ridges appear below the cliffs at the far end of the longitudinal hummocks (**Figure 4B**), and most of them are distributed in the intermediate transition zone and lateral edges of the accumulation area, and horizontal ridges are arranged in the way of parallel geese, showing the phenomenon of distortion or discontinuity in the same direction (**Figure 4A**).

The ridge landform unit of NRA is composed of a mixed clastic structure, which is not obviously different from mounds. It is surveyed that the formation of transverse ridges is related to the accumulation and compression of the basement, and the transverse ridges at the back of the central area are most developed; the original basement structure in this area is the transition zone between the accumulation of alluvial fans and the river peat swamp (**Figure 6E**), where the upper layer accumulation body develops debris jigsaw cracks. Therefore, it is speculated that the intrusion of the clastics is mainly horizontal displacement, and is mainly affected by the base structure. Although the sediments of the river marsh facies have finer grain size and the water content exceeds the proluvisis fan body, the gentle terrain is the main factor that causes the difference in fluid transportation speed, which leads to a

reduction in the speed of the front end of the transportation to make the rear side be squeezed in the horizontal direction.

4.3.3 Furrows and Trenches

The gully is an adverse linear terrain that regularly extends from the proximal end to the distal end. The gullies are densely developed in a nearly parallel arrangement from the middle to the distal area and extend along the main direction of transportation in a nearly parallel manner; in the central area, the length of the longest longitudinal gully is 0.6 km; and in the distal area, the gully is dense, and a part of the gully cuts off the longitudinal ridge at a short and sharp angle, forming densely arranged train hummocks (**Figure 4C**).

During the transportation, the flow is restricted by the base structure, resulting in differentiated transportation between blocks and causing stretching gully and shearing gully between blocks. By drawing the statistical map of the gully in different areas (**Figure 4A**), it is shown that the longitudinal gully is nearly parallel to the main transportation direction, and the horizontal gully is relatively underdeveloped. However, it turns into a conjugate gully form in the side edge area. At the front edge of the central zone, the extension of the gully is not straight.

From the topographic map based on DEM data (**Figure 4**), an arc-shaped gully spreading across the entire area along the front edge of the central area is clearly identified; besides, the river profile shows that a deformed basement facies is developed along the relatively open bottom of the gully. The basement layered sedimentary structure is inclined upstream due to the overlying pressure (**Figure 5B**), and the height of the ridge outside the gully has a significant step-like decline. It is inferred that the debris transportation in this area appears stretched and detached under the effect of the basement structure.

In the highest area in the central zone of the NRA, the developed shield-shaped mounds are formed by a set of conjugated gullies (Wang, et al., 2019), indicating the difference in the forces of the blocks in the accumulation area. These two groups of intersecting gullies show the main force property of horizontal left-handed shear. However, the right side of the shield-shaped mound in the central zone inclines downward to the outside, and multiple parallel ploughing ridges are developed forward (**Figure 5B**), indicating that during fluid transportation along the main direction, restricted by the base, a set of force couple is formed at the right side, resulting in the whole left-handed shear, thus forming longitudinal ridges separated by nearly parallel gullies in the middle area of the whole.

4.4 Facies

Along with the bank slopes of the Xuqu River and the tributary Xigaqu River, the exposed continuous and complete cross-sections and longitudinal sections show the details of the NRA macro-sedimentary structure, which is the upper carapace facies, the jigsaw-fractured body facies including blocks facies, mixing facies, shear facies, and basal facies according to the sedimentary sequence. Through careful investigation, it is found that it is typical for the missing of some sedimentary sequences in different regions, and the sequence of sedimentary structure is related to the structural properties of the clastic flow and interaction between the structure of the basement during the emplacement process.

1) The carapace facies are distributed from the proximal end of the scar area to the middle of the accumulation area (**Figure 5C**). In the proximal longitudinal mound area, the carapace layer is formed by the giant breccia and the vast internal survivor puzzle fissure, which is composed of the large breccia body and strip structure. The conclusion about the source of the large breccia is that it mainly comes from the middle and upper part of the scar area, develops in a belt shape along the advancing direction (**Figure 5D**).

It is worth noting that the crustacean facies abruptly disappeared in the central area and concentrated in a slightly distant part (**Figure 4C**). Generally, the carapace facies of NRA are distributed in most areas; in the proximal region, the granular structure of the carapace facies is characterized by megabreccias, the thickness of the crustaceans is large, and the boundary between the crustaceans and the body facies is not obvious. Starting from the middle of the Xuqu River, along with the distal direction, the particle size of breccias in the crustacean facies gradually decreases and shows an apparent discontinuity in the transition area from the middle to the distal, and then is concentrated generated. The crustacean almost disappeared in the leading edge area at the distal end.

2) The body facies are the accumulation, whose different regions are composed of a matrix of granularity ranging from coarse grain to clay, as the main part of the NRA. Its secondary types include block facies, fragmented facies, and mixed facies. Jigsaw cracks developed in block facies and mixed facies exist in most areas and particle size scales (**Figure 5C**), and their transition relationship depends on the content of fine-grained breccia and the mixed base sediments.

The shear facies of NRA is well developed. In the near-source area, parallel multi-shear zones or imbricated shear zones are developed inside the clastic deposits at the edges (**Figure 6A**). From the central area to the distal area, the shear zones mainly develop in the mixed facies, base deposition layer or between them, bands of finely ground are formed in the shear zone with a bandwidth ranging from centimetres millimetres (**Figure 6B**).

The investigation shows that the shear facies of Nyexon rock avalanches are developed from the bottom of the body facies to almost all ranges and depths of the disturbed basement. In the remote area, the development of the shear zone is affected and controlled by laminar flow and is often associated with rheological facies inside the clastics (**Figure 6C**). However, it also appears in the fine-grained block facies or mixed facies at the bottom. Different from the above characteristics, the upper mixed facies is in sharp contact with the substrate contact zone. The thickness of the mixed facies usually ranges from a few centimeters to more than 2 m. Shear bands significantly develop between the substrate facies and the mixed facies and inside the mixed facies. The direction of the internal jigsaw cracks is consistent with the transportation direction, and the

TABLE 1 | Description of facies zone of the NRA deposit

Facies zone	Main structures	Description
Sb (Scar block facies)	Ridges	The surface deposits are mainly mixed with breccias at the bottom of the scar area and the left slope zone.
SP (Southern Proximal Longitudinal Hummocks Facies)	Ridges, hummocks levées, trenches	Longitudinal ridges up to 940 m long oriented mostly SSE; the trenches are up to 30 m long; the levées are up to 530 m long; composed of carapace surface facies and internal mixed phases; flood dike is composed of mixed bas phases
NP (Northern Proximal Longitudinal Hummock Facies)	Ridges, hummocks levées	Longitudinal ridges up to 590 m long oriented mostly SSE; mixed block phase is the primary internal structure. The levées are up to 530 m long; base phase is the main material composition
Cm (Central Mixed Facies)	Faults; trenches	Located in the central zone of the deposit, lack of mounds and ridges, faults up to 150 m, the faults trend SS; trenches up to 240 m, trenches trend ENE; the largest deposition thickness developed, mainly composed of base material mixing, lack of surface crustacean facies
NC (Northern Central Mixed facies)	Ridges, hummocks, faults	Mainly structure consists of ridges, hummocks extending in the direction of SEE and NEE, and faults in the direction of NEE. Ridges and hummocks are 10–15 m high. It is mainly composed of local surface layer carapace phase, internal breccia matrix, and basement mixed phase materials
SC (Southern Central Mixed facies)	Ridges, hummocks, faults	Dominated by the ridges and hummocks structure extending in the direction of NWW and NEE. The heights of ridges and hummocks are 5–12 m, and they are mainly composed of local surface carapace phase and internal breccia matrix and basement mixed phase materials
Dh (Distal facies)	Hummocks	Composed of horizontal ridges and hummocks extending in the SEE direction. Ridges and hummocks are 3–8 m high and mainly composed of mixed phase materials

occurrence of the shear zone is in the range of near-horizontal to steep upstream.

3) The basal facies of NRA can be categorized into two similar types of structures. In the proximal area, the base facies is the piedmont alluvial fan; the main material components include the silt and gravel layer developed along the slope and gently dipping bedding, and the matrix of mixing phenomena between the base sediment and the overlying clastic bottom. In the local area of the edge, the phenomenon of diapir and injections occurs (**Figure 6D**).

The sediment components in the central and remote areas include silty sands with horizontal bedding and organic-rich clay interlayers. The lateral change law of basement facies structure shows that this area is mainly the transitional sedimentary zone between the end facies of alluvial fans and swamp facies (partially peat swamp). Complex deformation structures are observed in the bottom sediments covered by debris in a remote area. Some pieces of sediment float under the fluid and flow to deform accordingly (**Figure 6B**). However, in the remote area, the deformation of the basement is limited to the too deep range, which is usually in the range of 2~4 m from the bottom of the riverbed; thus, the basement surface can maintain the original horizontal sedimentary structure and disturbance.

Phenomena rarely occur. Even under the bedding shear zone (**Figure 6F**), there is no evidence of deformation that occurs inside the thin layer of horizontally bedding silt clay (Zeng et al., 2020).

4.5 Sedimentary Unit Division

Through the careful geological survey, the NRA sedimentary structure and spatial distribution range are investigated and mapped in detail; the entire area covered by the rock avalanche is divided into eight different sedimentary units or facies belts. **Table 1** lists the basic characteristics of the main units.

5 DISCUSSION

5.1 Collapse Mechanism of NRA

Referring to the worldwide large rock avalanches, rock slides, or detrital avalanches, different excitation conditions can cause almost all types of slopes to collapse (Moore and Mathews, 1978; Voight, 1981; Voight et al., 1983; Voight and Elsworth 1997; Belousov et al., 1999; Siebert, 1996). Triggered by a strong earthquake, the collapse of the rock avalanche or detrital avalanche is often remarkable, which means that the triggering effect of a strong earthquake can cause more severe damage, long-distance, and multi-stroke transportation (Cheng and Tian, 2000; Hu et al., 2009). Although for the Nyexon rock avalanches, there is no specific evidence to prove the relationship between collapse and the earthquake excitation, including the surface rupture phenomenon or the relationship between the activation time of the seismogenic fault and the rockfall event, strong earthquakes in Angang graben and surrounding areas are recorded; furthermore, the existence of Nyexon rock avalanches and slope disaster groups (Zeng et al., 2020) can be used as a basis for strong earthquake triggering.

Some collapse modes concerning large-scale rock avalanches or clastic avalanches induced by strong earthquakes, including the collapse mechanism of pyroclastic avalanches, are proposed (Belousov et al., 1999; Bernard et al., 2009; Pollet and Schneider, 2004; Huang et al., 2012). Through a detailed investigation of the scar area and slope environment of the Nyexon rock avalanche, it is believed that the original bottom structure of the scar area is affected by the fault to form a relatively weak basement, and concentrated stress shear failure may occur under the superimposed action of the overlying stress. The current

spatial structure of the scar area is not a typical wedge-shaped body, so it is a reasonable explanation of the foundation breaking to cause the damage of the slope.

Through the analysis of the slope's advantageous fracture combination and potential block structure, it is inferred that during the earthquake, the first deformation and destruction of the basement can make the slope continue to extend backward in the compression-induced fracture mode and develops into a deep failure surface along the existing dominant steeply inclined fissure, which eventually occurs the decomposition and failure of the wedge-shaped body. Therefore, considering the rock mass structure in different areas of the original slope in the scar area and the existing failure boundary characteristics, the failure mode of the basement collapse becomes a more reasonable explanation than the wedge failure.

5.2 Suggestion for the Mode of Rock Avalanche-Detrital Avalanche

Generally, the sedimentary structure of rock slip and rock avalanche is similar; they both include carapace facies, body facies, mixed facies, and basement facies, while the detrital avalanche lacks crustacean facies (Dufresne et al., 2015).

Through observation, in the proximal area of the Nyexon Rock avalanche, the main transported structure is mainly composed of incompletely broken breccia matrix and huge local survivors. Under the action of eroded or plow cutting, the basement layer occurs great deformation, where the development of the mixing facies is in the initial stage. Later, as the transportation distance increases to the remote area, the mixing facies becomes more mature, the development degree of the shear zone in the base and the mixing facies corresponds to its development stage; at the same time, the main body of transportation gradually turns to be the debris avalanche mode, in which the internal compression and collision behavior of the debris is more prominent. Moreover, some studies define this state as a particle flow (Friedmann, 2003; Hungr and Evans 2004).

On the other hand, with the lateral expansion, the degree of lateral expansion of clastic avalanches in the distal region is smaller than that of rock slides and rock avalanches. According to the plane evolution morphology, comparing to the Luanshibao Landslide and Taheman Landslide on the eastern edge of the Qinghai-Tibet Plateau while transporting open and flat terrain (Wang et al., 2019; Wang, ea al., 2020; Zeng et al., 2020), the lateral expansion of the Nyexon rockfall accumulation area is found to be not significant.

Based on the analysis above, it is believed that except for the evolution of the crustaceans, the Nyexon rock avalanche shows the evolution model of the detrital avalanche. According to the accumulation characteristics, the Nyexon rock avalanche enters the evolution mode of the detrital avalanche at the initial stage after the collapse; at this stage, the fragmentation process is obviously different from that of many other large rock avalanches during transportation, this may be an important aspect of the dynamic conditions for long distance transportation of rock avalanches, which also proves that different slide conditions may lead to significant differences in the mechanism of rockslide motion (Strom and Korup, 2006).

5.3 Facies Model of Rock Avalanches Deposition

Through the investigation of the sedimentary structure in different regions, it is found that there is a strong relationship between the accumulation morphology and sedimentation of the Nyexon rock avalanche. Many previous studies on the sedimentological characteristics of the rock avalanche are reflected by the facies model (Yarnold and Lombard, 1989; Pollet and Schneider, 2004; Dufresne et al., 2015).

Regarding the internal characteristics of the rock avalanche sedimentary structure, the vertical distribution of the clastic grain with size accumulation forms in different regions is studied and believed that the reverse hierarchical feature is for the upper sedimentary structure (Dunning, 2011; Weidinger et al., 2014). In the investigation of the Nyexon rock avalanche, most of the reverse grain structure is found to be in the mound section of the distal area (Wang et al., 2019), in which the impression of the reverse grain structure is further deepened because of the adding of the fine-grained basement material. The reverse structure is only developed inside the multi-shear zone or imbricate shear zone in the edge section in the proximal area. Therefore, the local reverse particle size of the rock avalanche is mainly related to the shearing mechanism. In this case, there is no direct field basis to support the vibration screening mechanism.

On the other hand, the reverse grain size in the NRA sedimentary structure is often closely related to the shear zone and its internal jigsaw cracks. The few jigsaw cracks in the near-source area of the NAR reflects scale benefits, which means that the larger survivors are wrapped in the early period. Even if the substrate is mixed or internally deformed, the influence of the surrounding stress concentration is not obvious. The jigsaw cracks appear more in the smaller-scale breccia matrix or a mixed belt in the distal area.

The development of shear bands represents the nature of fluid transport. In the proximal region, the shear bands mainly exist inside the substrate bottom, while they can further extend to the bottom or lower structure of mixed facies and body facies in the distal region. At the bottom of the hill or ridge section, there is a gentle bottom mixing zone and the basement interface that does not match the surface morphology, and in some areas also occurs a certain degree of uplift, forming rheological formation and shear zones.

According to the detailed discussion of the spatial distribution and internal structure of the various sedimentary facies during the placement of the NRA, the mode of sedimentary facies of the NRA is drawn (**Figure 7**).

5.4 Rockfall Dynamics and Emplacement Restraint Mechanism

As mentioned in a previous section (**Section 5.1**), in the initial stage after the collapse of the NRA, the main transport structure is dominated by mixed giant breccias and debris but lacks the original structure and strength. At the same time, the substrate containing viscous materials is not added, it is defined as a non-aqueous and non-sticky granular material and keeps the particle flow

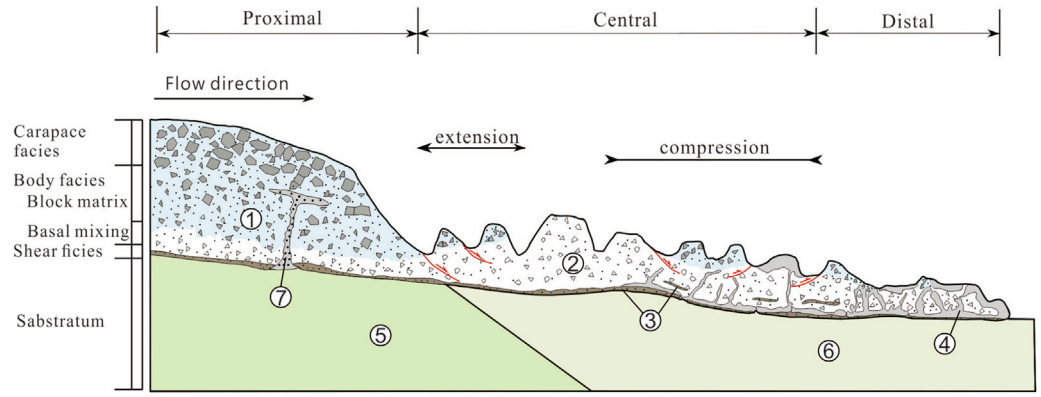

FIGURE 7 | The facies model of Nyexon rock avalanches. (1) Block facies; (2) mixed facies; (3) shear facies; (4) fine grained mixing facies; (5) and (6) substratum of differentiation; (7) basel injection.

properties during the transportation. In the proximal region, the debris particles are transported in the form of flow, and the intrusion process causes the deformation of the substrate. The structure of longitudinal hummocks and dams is related to the stretching mechanism of the fluid in the slope zone (Wang et al., 2019), which is related to some other debris avalanches. However, corresponding to the limited conditions of the original lateral ridge, the transportation direction of the fluid in the vicinity of the edge is different from the middle fluid. After the collapse of the scar area, the initial transportation state is the main factor in controlling the transportation direction. When the longitudinal mound in the left area is under the combined influence of the lateral constraint and the deformation of the substrate, the transportation of the fluid front decelerates and a key terrain obstacle is formed behind the transverse ridge of the central zone (the central area in **Figure 4**); after arriving, the middle area, affected by the obstacle heights, the transportation direction of the fluid furtherly changes from 103° to 155°. Finally, the fluid continues to run off and expand downstream, forming the current planar shape.

Although the bottom of the basin has the characteristics of open and flat primitive landforms, the flow of rock avalanches has inherited characteristics. The fluid entering the bottom of the basin from the slope zone is affected by the transformation of the substrate structure and friction properties. In order to quantify the impact, the macroscopic friction coefficients generated by rock slides at the interface of different substrate is calculated using two different sections (**Figure 2**), and the results calculated by applying the formula Δh/L (Ui, 1983) are respectively 0.18 and 0.23, indicating that the friction coefficient of the substrate of the slope-diluvial fan is much higher than that of the swamp substrate, and it also shows that the NRA is similar to some other rock avalanches or clastic avalanches (Siebert, 1984; Shaller, 1991), it is not an abnormal long-distance transportation.

According to the previous description, hills or ridges are not formed by the deformation and undulation of the basement regarding the long-distance transportation mechanism of rock avalanches at the bottom of river valleys. However, they are mainly related to the compression and extension of the fluid. From the central area to the distal area, the mixed facies and shear zone mainly develop in the bottom area of the fluid, where the fluid structure and density change the most. The investigation of the NRA shows that the fluid intrusion in the remote area is mainly in the form of destruction of the shear zone rather than theology, and the bottom mixing zone rich in fine-grained materials has a lower porosity. The swamp sediments of the basal facies have finer grain size and are saturated with water. During the fluid emplacement process, the substrate underwent most of the shear failure under the action of excess pore water pressure. In addition, along the basal facies or the mixed-facies structure is a mainly laminar failure, and a small part of the outside of the central area is the shear failure inside the mixed facies, forming an inclined failure surface that is nearly parallel to the surface of the mound.

In the distal and lateral areas, the fluid becomes abnormally thin, and the shear band does not move down significantly, indicating that the internal shear of the fluid is not directly related to the overlying pressure determined by the fluid thickness, so it can be inferred that the shearing is the reason for inheriting the weak zone or shear zone that existed before the lateral expansion.

6 CONCLUSION

In this paper, the Nyexon rock avalanche in Nyemo County, southern Tibet, was studied, formed inside the Angang graben under strong earthquakes. The debris formed after rock avalanche damage is transported from the gentle slope belt in front of the mountain to the flat and open lower reaches of the Angang River valley, during which the transport direction of the rock avalanche abnormally changes; this makes the Nyexon avalanche be a specific case of studying the failure mechanism and intrusion constraints of large rock avalanches. Finally, some new understandings and summaries were obtained based on detailed geological observations and previous studies.

1) The collapse and failure mode of the Nyexon rock avalanche the foundation failure after the earthquake stress is

superimposed on the weak foundation that is formed under the control of the fracture in the bottom area of the slope under the action of strong earthquakes, and after its strong collision with the bottom surface and caused rapid fragmentation, the rock mass in the scar area is broken and decomposed to form the initial condition for rockfall debris to be transported by particle flow.

2) The original slope landform and basement sedimentary structure are different from previous understandings. The basement of lateral ridges and piedmont gentle slopes is composed of slope alluvial materials, while the bottom of the Angang River valley is composed of river-swamp facies. The difference in sedimentary structure has obvious influence on the transportation and intrusion of rock avalanche.
3) Through the investigation and analysis of the morphology and structure of the rock avalanche accumulation area, the established Nyexon rock avalanche sedimentary facies model includes: 1) block facies and disturbed basement facies in the proximal area after initial fragmentation; 2) the rheology of the block facies, the mixed facies, and the base liquefaction facies in the central area; 3) the base facies and shear zone in the distal region; 4) under tension and compression, the formed surface morphology corresponding to the hills, ridges, and ravines; and 5) radial transportation based on horizontal shear zone.
4) The collapse and disintegration process of the slope in the source area resulted in the separation of the clastic fluid during the longitudinal transportation, and under the condition of the lateral and base boundary being constrained, the deceleration of the fluid transportation forms the high obstacle land in the central area, forcing the intrusion direction to be obviously deflected, which is the main development process of the overall plane morphology of the NRA.

Due to the complexity of the long-distance transportation process of the NRA, it is necessary to study the excitation of strong earthquakes to reveal the mechanism of earthquake action on the slope scar area, and further clarify the inner relationship between the debris intrusion process and the sedimentary structure after rock avalanche failure.

DATA AVAILABILITY STATEMENT

The original contributions presented in the study are included in the article/Supplementary Material. Further inquiries can be directed to the corresponding author.

AUTHOR CONTRIBUTIONS

CG: Conceptualization, methodology. JC: Data curation, writing, original draft preparation. ZZ: Reviewing and editing, investigation. GX: Validation. XL: Visualization. YH: Resources.

FUNDING

This research was funded by the National Key Research and Development Project of China (No. 2018YFC1505000).

ACKNOWLEDGMENTS

Thank you very much to Deng Jianhui of Sichuan University, Wen Baoping of China University of Geosciences (Beijing), and Dai Fuchu of Beijing University of Technology for their guidance.

REFERENCES

Anma, S., Maikuma, H., Yoshimura, M., Fujita, Y., and Okusa, S. (1989). Dynamics of Earthquake-Induced Slope Failure of Ontake. *Int. J. Rock Mech. Mining Sci. Geomechanics Abstr.* 26 (2), 89. doi:10.1016/0148-9062(89)90312-4

Armijo, R., Tapponnier, P., Mercier, J. L., and Han, T. (1986). Quaternary Extension in Southern Tibet: Field Observations and Tectonic Implications. *J. Geophys. Res. Solid Earth* 91 (B14), 13803. doi:10.1029/jb091ib14p13803

Belousov, A., Belousova, M., and Voight, B. (1999). Multiple Edifice Failures, Debris Avalanches and Associated Eruptions in the Holocene History of Shiveluch Volcano, Kamchatka, russia. *Bull. Volcanology* 61 (5), 324–342. doi:10.1007/s004450050300

Bernard, B., van Wyk de Vries, B., Barba, D., Leyrit, H., Robin, C., Alcaraz, S., et al. (2008). The Chimborazo Sector Collapse and Debris Avalanche: deposit Characteristics as Evidence of Emplacement Mechanisms. *J. Volcanology Geothermal Res.* 176 (1), 36–43. doi:10.1016/j.jvolgeores.2008.03.012

Capra, L., MaciÂs, J. L., Scott, K. M., Abrams, M., and Garduño-Monroy, V. H. (2002). Debris Avalanches and Debris Flows Transformed from Collapses in the Trans-Mexican Volcanic Belt, Mexico-Behavior, and Implications for Hazard Assessment. *Journal of Volcanology and Geothermal Research* 113 (1), 81–110.

Cheng, Q. G., and Tian, H. H. (2000). *Discrete Element Simulation of Full Course Kinematics of Rocky High Speed Landslide*. Journal of Southwest Jiaotong University.

Clavero, J., Sparks, R., Huppert, H., and Dade, W. (2002). Geological Constraints on the Emplacement Mechanism of the Parinacota Debris Avalanche, Northern chile. *Bull. Volcanology* 64 (1), 40–54. doi:10.1007/s00445-001-0183-0

Davies, T. R., Mcsaveney, M. J., and Hodgson, K. A. (1999). A Fragmentation-Spreading Model for Long-Runout Rock Avalanches. *Can. Geotech. J.* 36 (6), 1096–1110. doi:10.1139/t99-067

Davies, T. R. H. (1982). Spreading of Rock Avalanche Debris by Mechanical Fluidization. *Rock Mech.* 15 (1), 9–24. doi:10.1007/bf01239474

Dufresne, A., and Davies, T. R. (2009). Longitudinal Ridges in Mass Movement Deposits. *Geomorphology* 105 (3-4), 171–181. doi:10.1016/j.geomorph.2008.09.009

Dufresne, A., Prager, C., and Clague, J. J. (2015). *Complex Interactions of Rock Avalanche Emplacement with Fluvial Sediments: Field Structures at the Tschirgant Deposit*. Austria: Springer International Publishing.

Dunning, S. (2011). *The Grain-Size Distribution of Rock-Avalanche Deposits: Implications for Natural Dam Stability*. Springer Berlin Heidelberg.

Erismann, T. H., and Abele, G. (2001). *Dynamics of Rockslides and Rockfalls*.

Erismann, T. H. (1979). Mechanisms of Large Landslides. *Rock Mech.* 12 (1), 15–46. doi:10.1007/bf01241087

Evans, S. G., Clague, J. J., Woodsworth, G. J., and Hungr, O. (1989). The Pandemonium Creek Rock Avalanche, British columbia. *Int. J. Rock Mech. Mining Sci. Geomechanics Abstr.* 27 (2), A112. doi:10.4095/130685

Evans, S. G. (1989). Rock Avalanche Run-Up Record. *Nature* 340 (6231), 271. doi:10.1038/340271a0

Friedmann, S., J. (2003). Granular Memory and its Effect on the Triggering and Distribution of Rock Avalanche Events. *J. Geophys. Res. Solid Earth* 108 (B8). doi:10.1029/2002jb002174

Guitang, P., Xuanxue, M. O., Hou, Z. Q., et al. (2006). Spatial-temporal Framework of the Gangdese Orogenic Belt and its Evolution. *Acta Petrologica Sinica* 22 (3), 521–533.

Hewitt, K. (1999). Quaternary Moraines vs Catastrophic Rock Avalanches in the Karakoram Himalaya, Northern pakistan. *Quat. Res.* 51 (3), 220–237. doi:10.1006/qres.1999.2033

Hsü, K. J. (1975). Catastrophic Debris Streams (Sturzstroms) Generated by Rockfalls. *Geol. Soc. America Bull.* 86 (1), 129. doi:10.1130/0016-7606(1975)86<129:cdssgb>2.0.co;2

Hu, M., Cheng, Q., and Wang, F. (2009). Experimental Study on Formation of Yigong Long-Distance High-Speed Landslide. *Chin. J. Rock Mech. Eng.* 28 (1), 138–143.

Hu, G. (1995). *Landslide Dynamics*, 1. Beijing: Geology publishing house, 6–22.

Huang, R., Pei, X., Fan, X., Zhang, W., Li, S., and Li, B. (2012). The Characteristics and Failure Mechanism of the Largest Landslide Triggered by the Wenchuan Earthquake, May 12, 2008, china. *Landslides* 9 (1), 131–142. doi:10.1007/s10346-011-0276-6

Hungr, O., and Evans, S. G. (2004). Entrainment of Debris in Rock Avalanches: an Analysis of a Long run-out Mechanism. *Geological Society of America Bulletin* 116 (9-10), 1240–1252.

Jibson, R. W., Harp, E. L., Schulz, W., and Keefer, D. K. (2006). Large Rock Avalanches Triggered by the M 7.9 Denali Fault, alaska, Earthquake of 3 November 2002. *Eng. Geology.* 83 (1-3), 144–160. doi:10.1016/j.enggeo.2005.06.029

Kent, P. E. (1966). The Transport Mechanism in Catastrophic rock falls. *J. Geology.* 74 (1), 79–83. doi:10.1086/627142

Moore, D. P., and Mathews, W. H. (1978). The Rubble Creek Landslide, Southwestern British Columbia. *Can. J. Earth Sci.* 15 (7), 1039–1052. doi:10.1139/e78-112

OldrichHungr, S. G. E. (2004). *Entrainment of Debris in Rock Avalanches: An Analysis of a Long Run-Out Mechanism*. Geological Society of America Bulletin.

Orwin, J. F., Clague, J. J., and Gerath, R. F. (2004). The Cheam Rock Avalanche, Fraser Valley, British Columbia, Canada. *Landslides* 1 (4), 289–298. doi:10.1007/s10346-004-0036-y

Pier, G., Nicoletti, P. G., and Sorriso-Valvo, M. (1991). Geomorphic Controls of the Shape and Mobility of Rock Avalanches. *Geol. Soc. America Bull.* 103 (10), 1365–1373. doi:10.1130/0016-7606(1991)103<1365:gcotsa>2.3.co;2

Pollet, N., and Schneider, J. (2004). Dynamic Disintegration Processes Accompanying Transport of the Holocene Flims Sturzstrom (Swiss Alps). *Earth Planet. Sci. Lett.* 221 (1-4), 433–448. doi:10.1016/s0012-821x(04)00071-8

Qi, S., Xu, Q., Zhang, B., Zhou, Y., Lan, H., and Li, L. (2011). Source Characteristics of Long Runout Rock Avalanches Triggered by the 2008 Wenchuan Earthquake, china. *J. Asian Earth Sci.* 40 (4), 896–906. doi:10.1016/j.jseaes.2010.05.010

Qiang, X., Shang, Y., Asch, T. V., Wang, S., Zhang, Z., and Dong, X. (2012). Observations from the Large, Rapid Yigong Rock Slide–Debris Avalanche, Southeast Tibet. *Revue Canadienne De Géotechnique* 49 (5), 589–606.

Sassa, K. (1988). Geotechnical Model for the Motion of Landslides (Special Lecture). *Proĉ Int.symp.on Landslides* 26 (2), 88. doi:10.1016/0148-9062(89)90311-2

Schilirò, L., Esposito, C., Blasio, F. V. D., and Mugnozza, G. S. (2019). Sediment Texture in Rock Avalanche Deposits: Insights from Field and Experimental Observations. *Landslides* 16 (1160), 1–15. doi:10.1007/s10346-019-01210-x

Shaller, P. J. (1991). Analysis of a Large Moist Landslide, Lost River Range, idaho, u.s.a. *Can. Geotech. J.* 28 (4), 584–600. doi:10.1139/t91-073

Shreve, R. L. (1966). Sherman Landslide, alaska. *Science* 154 (3757), 1639–1643. doi:10.1126/science.154.3757.1639

Siebert, L. (1984). Large Volcanic Debris Avalanches: Characteristics of Source Areas, Deposits, and Associated Eruptions. *J. Volcanology Geothermal Res.* 22 (3-4), 163–197. doi:10.1016/0377-0273(84)90002-7

Siebert, L. (1996). *Hazards of Large Volcanic Debris Avalanches and Associated Eruptive Phenomena*. Springer Berlin Heidelberg.

Strom, A. L., and Korup, O. (2006). Extremely Large Rockslides and Rock Avalanches in the Tien Shan Mountains, kyrgyzstan. *Landslides* 3 (2), 125–136. doi:10.1007/s10346-005-0027-7

Takarada, S., Ui, T., and Yamamoto, Y. (1999). Depositional Features and Transportation Mechanism of Valley-Filling Iwasegawa and Kaida Debris Avalanches, Japan. *Bulletin of Volcanology* 60 (7), 508–522.

Tapponnier, P., Ryerson, F. J., Van der Woerd, J., Mériaux, A.-S., and Lasserre, C. (2001). Long-term Slip Rates and Characteristic Slip: Keys to Active Fault Behaviour and Earthquake hazard. *Comptes Rendus de l'Académie des Sci. - Ser. IIA - Earth Planet. Sci.* 333 (9), 483–494. doi:10.1016/s1251-8050(01)01668-8

Taylor, M., Yin, A., Ryerson, F. J., Kapp, P., and Ding, L. (2003). Conjugate Strike-Slip Faulting along the Bangong-Nujiang Suture Zone Accommodates Coeval East-West Extension and north-south Shortening in the interior of the Tibetan Plateau. *Tectonics* 22 (4), 1044–1068. doi:10.1029/2002tc001361

Vallance, J. W., and Scott, K. M. (1997). The Osceola Mudflow from Mount Rainier: Sedimentology and Hazard Implications of a Huge Clay-Rich Debris Flow. *Geological Society of America Bulletin* 109 (2), 143–163.

Voight, B., and Elsworth., D. (1997). *Failure of Volcano Slopes*. Geotechnique.

Voight, B., Janda, R. H., Glicken, H. X., and Douglass, P. M. (1983). Nature and Mechanics of the Mount St. Helens Rockslide-Avalanche of 18 May 1980. *Géotechnique* 33 (3), 357–368. doi:10.1680/geot.1983.33.3.243

Voight, B. (1981). Catastrophic Rockslide Avalanche of May 18. *U.s.g.s.professional Paper* 1250 (9), 347–377. doi:10.3133/ofr96677

Wang, Y.-F., Cheng, Q.-G., Lin, Q.-W., Li, K., and Yang, H.-F. (2018). Insights into the Kinematics and Dynamics of the Luanshibao Rock Avalanche (Tibetan Plateau, china) Based on its Complex Surface Landforms. *Geomorphology* 317, 170–183. doi:10.1016/j.geomorph.2018.05.025

Wang, Y.-F., Cheng, Q.-G., Shi, A.-W., Yuan, Y.-Q., Qiu, Y.-H., and Yin, B.-M. (2019). Characteristics and Transport Mechanism of the Nyixoi Chongco Rock Avalanche on the Tibetan Plateau, china. *Geomorphology* 343 (Oct.15), 92–105. doi:10.1016/j.geomorph.2019.07.002

Wang, Y.-F., Cheng, Q.-G., Yuan, Y.-Q., Wang, J., Qiu, Y.-H., Yin, B.-M., et al. (2020). Emplacement Mechanisms of the Tagarma Rock Avalanche on the Pamir-Western Himalayan Syntaxis of the Tibetan Plateau, china. *Landslides* 17 (3), 527–542. doi:10.1007/s10346-019-01298-1

Wang, Y. F., Dong, J. J., and Cheng, Q. G. (2017). Velocity-Dependent Frictional Weakening of Large Rock Avalanche Basal Facies: Implications for Rock Avalanche Hypermobility?. *Journal of geophysical research. Solid earth: JGR* 122 (3), 1648–1676.

Weidinger, J. T., Korup, O., Munack, H., Altenberger, U., Dunning, S. A., Tippelt, G., et al. (2014). Giant Rockslides from the inside. *Earth Planet. Sci. Lett.* 389, 62–73. doi:10.1016/j.epsl.2013.12.017

Wu, Z. H., and Ye, P. S. (2009). The Seismic Intensity, Seismogenic Tectonics and Mechanism of the Ms6.6 Damxung Earthquake Happened on October 6,2008 in Southern Tibet,China. *Geol. Bull. China* 28 (6), 713–725.

Wu, Z., Ye, P., Wang, C., Zhang, K., and Li, H. (2015). The Relics,ages and Significance of Prehistoric Large Earthquakes in the Angang Graben in South Tibet. *Earth ence(Journal China Univ. Geoences)* 40 (10), 1621–1642.

Yarnold, J. C., and Lombard, J. P. (1989). *Facies Model for Large Rock Avalanche Deposits Formed in Dry Climates*. pacific.

Yin, A., and Taylor, M. H. (2011). Mechanics of V-Shaped Conjugate Strike-Slip Faults and the Corresponding Continuum Mode of continental Deformation. *Geol. Soc. America Bull.* 123 (9-10), 1798–1821. doi:10.1130/b30159.1

Zeng, Q., Wei, R., Mcsaveney, M., Ma, F., and Liao, L. (2020). From Surface Morphologies to Inner Structures: Insights into Hypermobility of the Nyexon Rock Avalanche, Southern Tibet, china. *Landslides* 18 (1-2), 125–143. doi:10.1007/s10346-020-01503-6

Conflict of Interest: The authors declare that the research was conducted in the absence of any commercial or financial relationships that could be construed as a potential conflict of interest.

Publisher's Note: All claims expressed in this article are solely those of the authors and do not necessarily represent those of their affiliated organizations, or those of the publisher, the editors, and the reviewers. Any product that may be evaluated in this article, or claim that may be made by its manufacturer, is not guaranteed or endorsed by the publisher.